

# Peak infection rate in epidemic spreading for multi-community networks

Jing Ma,<sup>1,\*</sup> Xiangyi Meng,<sup>2</sup> and Lidia A. Braunstein<sup>3,1</sup>

<sup>1</sup>*Department of Physics, Boston University, Boston, MA 02215, USA*

<sup>2</sup>*Center for Complex Network Research and Department of Physics, Northeastern University, Boston, MA 02115, USA*

<sup>3</sup>*Instituto de Investigaciones Físicas de Mar del Plata (IFIMAR), FCEyN, Universidad Nacional de Mar del Plata-CONICET, Déan Funes 3350, (7600) Mar del Plata, Argentina*

## Abstract

One of the most effective strategies to mitigate the global spreading of a pandemic (e.g., COVID-19) is to shut down international airports. From a network theory perspective, this is since international airports and flights, essentially playing the roles of bridge nodes and bridge links between countries as individual communities, dominate the epidemic spreading characteristics in the whole multi-community system. Among all epidemic characteristics, the peak infection rate,  $I_{\max}$ , is a decisive factor in evaluating an epidemic strategy given limited capacity of medical resources, but is seldom considered in multi-community models. In this paper, we study a general two-community system interconnected by a fraction  $r$  of bridge nodes and its dynamic properties, especially  $I_{\max}$ , under the evolution of the Susceptible-Infected-Recovered (SIR) model. Comparing the characteristic time scales of different parts of the system allows us to analytically derive the asymptotic behavior of  $I_{\max}$  with  $r$ , as  $r \rightarrow 0$ , which follows different power-law relations in each regime of the phase diagram. We also detect crossovers where  $I_{\max}$  follows power-law relations from different regimes on both sides, when  $r$  is not small enough. Our results enable a better prediction of the effectiveness of strategies acting on bridge nodes, denoted by the power-law exponent  $\epsilon_I$  as in  $I_{\max} \propto r^{1/\epsilon_I}$ .

---

\* jingma@bu.edu

## I. INTRODUCTION

Network science has provided many useful tools for studying epidemic problems [1]. By modeling an epidemic-confronting society as a network, where each individual is modeled as a node and every infectious interaction between two individuals as a link, an epidemic problem can often be reduced to a pure problem of percolation theory and network dynamics which strongly depend on the network topology. In many synthetic and real-world complex networks, it is known that the number of short loops is negligible [2], and thus the network topology can be characterized by two generating functions  $G_0$  and  $G_1$  denoting the *degree distribution* and the *excess degree distribution*:  $G_0(x) = \sum_k P(k)x^k$  and  $G_1(x) = \langle k \rangle^{-1} \sum_k kP(k)x^{k-1}$ , respectively, given  $P(k)$  the fraction of nodes of degree  $k$  in the network [3, 4].

In the Susceptible-Infected-Recovered (SIR) model, the course of a disease can be modeled as three states, and each individual can be in one of these three states at any instant: susceptible (S, i.e., not infected yet), infected (I), and recovered (R). An individual will recover  $t_r$  time steps after being infected, and is then immune to the disease and will never get infected again. It has been well known that the final steady state of the SIR model can be mapped into a link percolation problem [5–7]. In this mapping, the fraction of individuals that have ever been infected at the final state  $R_{\text{final}}$  is just the size of the cluster that patient zero belongs to in the link percolation problem, which is the order parameter of a phase transition; the transmissibility  $T$  in the SIR model, which is the probability that an infected node can spread this disease to its neighbor through a link before it recovers, is equivalent to the probability of a link being occupied in the link percolation problem, which is the control parameter.

In recent years, there are many studies about epidemics in multi-community systems. In such kind of systems, each community is itself a complex network of some degree distribution, while multiple communities are coupled to each other through either shared nodes [8, 9] or bridge links that follow a possibly different degree distribution [10–13]. In a system of multiple communities connected by bridge links, which allows for different transmissibilities along internal links ( $T^i$ ) and bridge links ( $T^b$ ), it has been shown that  $R_{\text{final}}$  asymptotically follows different power-law behaviors with  $r$  in different regimes, where  $r$  is the fraction of nodes in the whole system that are bridge nodes [14]. These results enable better decisions

about epidemic strategies such as whether social distancing strategies are needed (to reduce transmissibility  $T$ ) or how many international airports need to be closed (to reduce the fraction of bridge nodes  $r$ ).

Besides the final steady state  $R_{\text{final}}$ , the dynamic properties of the SIR process, especially the peak infection rate  $I_{\text{max}}$ , are also of great interest. The dynamics of SIR has been well known to belong to the same dynamic universality class of link percolation, given its equivalence to the breadth-first process (the Leath-Alexandrowicz algorithm [15, 16]) that is used for simulating the growth of percolation clusters [17]. In this paper, instead of looking at the final state of SIR, we study its dynamic properties in a two-community system with bridge links. By comparing the time scale of different parts of the system, we find that the peak infection rate  $I_{\text{max}}$  also follows different power laws with the fraction of bridge nodes  $r$  in different regimes as  $r \rightarrow 0$ . The regimes are determined by the comparison between the order parameters ( $T^i$  and  $T^b$ ) and their critical values in isolated systems, while the exponents in different regimes are related to the exponents for  $R_{\text{final}}$ , which were found in Ref. [14]. All of our results are verified by numerical simulations. Together with Ref. [14], our results now can predict not only the total number of patients in the SIR model, but also the maximum number of patients during the epidemic. In practice,  $I_{\text{max}}$  is a more decisive factor, as it actually decides the transient maximum capacity of patients who can receive timely treatment.

## II. MODEL

Consider a system of two communities  $A$  and  $B$ , where a fraction  $r$  of nodes from each community are *bridge nodes*, between which *bridge links* that interconnect  $A$  and  $B$  exist. The subsystem composed of bridge nodes and bridge links is denoted by  $b$ , as shown in Fig. 1. For simplicity, we assume the two communities  $A$  and  $B$  are statistically identical, so that  $P^A(k) = P^B(k) \equiv P^i(k)$ , and that the internal transmissibility is also the same within each community, given by  $T^A(k) = T^B(k) \equiv T^i(k)$ . The bridge links are allowed to have a different degree distribution  $P^b(k)$  and a different transmissibility  $T^b$ . Note that all the methods and results in this paper can be generalized to cases with  $P^A(k) \neq P^B(k)$  and/or  $T^A \neq T^B$ .

The step-by-step evolution of the system can then be simulated by the Edge-Based Com-

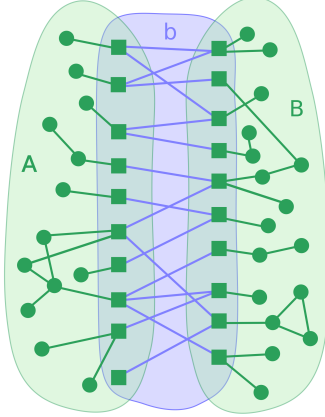


FIG. 1: Illustration of a two-community system composed by communities  $A$  and  $B$ . The subsystem  $b$  is composed of bridge nodes and bridge links. Bridge nodes are denoted by squares and internal nodes by circles.

partmental Model (EBCM) adapted to the SIR model [18, 19]. As a mean-field model, the EBCM is a set of difference equations that can reproduce the evolution of disease spreading using much less time than calculating the states of all nodes individually at each time step (see Appendix A). For example, in a two-community system where both internal and bridge links follow Poisson distributions  $P(k) = \langle k \rangle^k e^{-\langle k \rangle} / k!$ , with  $\langle k^i \rangle = 4$ ,  $\langle k^b \rangle = 10$ ,  $r = 0.1$ ,  $T^i = 0.5$ ,  $T^b = 0.2$ , the time dependence of  $S$ ,  $I$ ,  $R$  based on the EBCM simulation [Eqs. (2)-(11)] shows that  $R$  will increase from zero and then stabilize to a value  $R_{\text{final}}$ , and that  $I$  will increase at the beginning but then decrease after passing a peak value  $I_{\text{max}}$  (Fig. 2). It has been studied in Ref. [14] that  $R_{\text{final}}$  has different power-law behaviors with  $r$  in different regimes. In this paper, we will show that  $I_{\text{max}}$  also follows power-law relations with  $r$  as  $r \rightarrow 0$ , and that crossovers exist between some regimes when  $r$  is not small enough.

### III. ASYMPTOTIC DEPENDENCE OF $I_{\text{max}}$ ON $r$ IN DIFFERENT REGIMES

By mapping the SIR model to a link percolation problem, we can apply well-known results of percolation theory to epidemic problems. Hence, we are going to use the terminologies in the SIR model and percolation theory interchangeably. In the SIR model, the critical value of transmissibility in an isolated network is given by  $T_c = 1/(\kappa - 1)$ , where  $\kappa = \langle k^2 \rangle / \langle k \rangle$  is the branching factor [20, 21]. This critical point is characterized by many behaviors, e.g.,

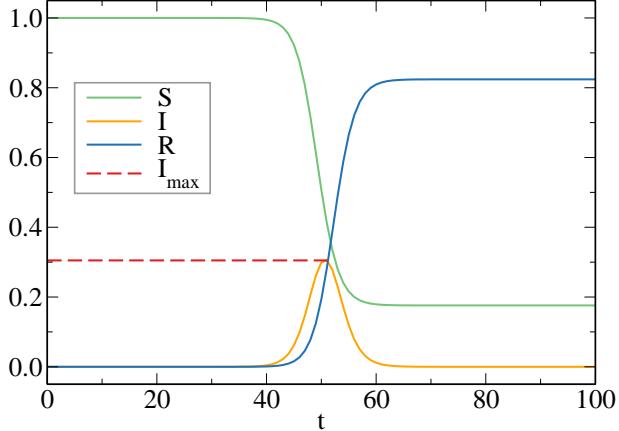


FIG. 2: Time dependence of the susceptible (S), infected (I), and recovered (R) in the SIR model in a two-community system, where both internal and bridge links follow Poisson distributions, with  $\langle k^i \rangle = 4$ ,  $\langle k^b \rangle = 10$ ,  $r = 0.1$ ,  $T^i = 0.5$ ,  $T^b = 0.2$ .

the probability to find a cluster of size  $s$  is given by  $P(s) \sim s^{-\tau+1} \exp(-s/s_{\max})$ , where  $s_{\max} \sim |T - T_c|^{-1/\sigma}$  is the largest finite cluster size [6, 22]. For Erdős-Rényi (ER) networks whose degree distribution follows a Poisson distribution  $P(k) = \langle k \rangle^k e^{-\langle k \rangle} / k!$ , we always have  $\tau = 5/2$ ; for scale-free (SF) networks where the degree distribution is a power law  $P(k) \propto k^{-\lambda}$  with  $3 < \lambda < 4$ ,  $\tau$  is given by  $\tau = (2\lambda - 3)/(\lambda - 2)$  [23]. Also, the correlation length  $\xi$  diverges around the critical point following  $\xi \sim |T - T_c|^{-\nu}$ , where  $\nu = 1/2$  for both ER and SF networks. There are also dynamic behaviors around the critical point, e.g., the chemical distance  $l$ , which represents the time scale in epidemic models [24], is related to the correlation length  $\xi$  by  $l \sim \xi^z \sim |T - T_c|^{-z\nu}$ , in which  $z = 2$  for both ER and SF networks.

Due to the abrupt change in behaviors around the critical points, we are going to split the space of the combination of  $T^i$  and  $T^b$  into seven regimes, based on whether  $T^i$  is less than, equal to, or larger than  $1/(\kappa^i - 1)$ , and whether  $T^b$  is less than, equal to, or larger than  $1/(\kappa^b - 1)$ , in the same way as shown in the phase diagram (see Fig. 2 in Ref. [14]). Note that  $1/(\kappa^i - 1)$  or  $1/(\kappa^b - 1)$  is the critical value of  $T^i$  or  $T^b$  when the respective part is isolated. And we are going to look at the peak infection rate  $I_{\max}$  in each regime.

In order to derive the behavior of  $I_{\max}$ , it is helpful to denote  $I^b$  as the fraction of bridge nodes that are infected at any instant, and  $I_{\max}^b$  as the peak infection rate for bridge nodes. For a community, the peak infection rate  $I_{\max}$  is related to the status of its bridge nodes, i.e., either  $rR_{\text{final}}^b$  or  $rI_{\max}^b$ , where  $R_{\text{final}}^b$  is the fraction of bridge nodes that are recovered at

the final state, depending on whether they get infected within a small or large time scale. Specifically, if the time scale of a community is much less than the time scale of the whole system, the spreading of the disease in the community can be treated as multiple “breakouts” within the community occurring one after another, i.e., those “breakouts” will not overlap over time; on the other hand, if the time scale of a community is much larger than the time scale of the system, all the “breakouts” will keep spreading within the community and accumulate over time.

The dependencies of  $I_{\max}$  and  $I_{\max}^b$  in each regime are discussed separately as follows:

1. When  $T^i < 1/(\kappa^i - 1)$ , each community itself has a finite time scale. There are at most  $rI_{\max}^b$  infected bridge nodes at any instant, and each of them is expected to expand to a finite number of nodes within the community, since all clusters within each community are finite clusters below criticality. Consequently,  $rI_{\max}^b \leq I_{\max} \leq rI_{\max}^b \cdot s_{\max}$ , where  $s_{\max}$  is finite, so  $I_{\max} \propto rI_{\max}^b$ , as  $r \rightarrow 0$ , which is true for any value of  $T^b$ .

1.1 (Regime I) When  $T^b < 1/(\kappa^b - 1)$ , the whole system is in non-epidemic regime, so  $I_{\max}$  or  $I_{\max}^b$  is not a power law of  $r$ .

1.2 (Regime II) When  $T^b = 1/(\kappa^b - 1)$ , there is the relation  $R_{\text{final}}^b \sim I_{\max}^b \cdot l^b$  by dimensional analysis, where  $l^b$  represents the time scale of the bridge link part. Since  $l^b \sim |T^b - T_c^b|^{-z^b \nu^b} \sim |T^b - T_c^b|^{-1}$  given  $z = 2$  and  $\nu = 1/2$  for both ER and SF networks with  $3 < \lambda < 4$ , and also  $|T^b - T_c^b| \sim r$  where  $T_c^b$  is the critical value of bridge link transmissibility for the whole system given a fixed value of  $T^i$  (see Appendix B), we have  $I_{\max}^b \sim rR_{\text{final}}^b$ .

1.3 (Regime III) When  $T^b > 1/(\kappa^b - 1)$ , there is a giant component within the network of bridge links  $b$  in finite time steps, so  $I_{\max}^b$  is not a power law of  $r$ .

2. (Regime IV, V, VI) When  $T^i = 1/(\kappa^i - 1)$ , each community has an infinite time scale, while the whole system has a finite time scale. There are  $rR_{\text{final}}^b$  bridge nodes being infected in total, and they get infected within a short period of time due to the finite time scale of the system. This is equivalent to considering that there are  $rR_{\text{final}}^b$  bridge nodes that get infected at the same time, and they are going to spread the disease within each community, so it is expected that there are at most  $I_{\max} \propto rR_{\text{final}}^b$  nodes that are being infected at the same time (see Appendix C).

3. (Regime VII) When  $T^i > 1/(\kappa^i - 1)$ , there is always a giant component within each community, and thus always a finite  $I_{\max}$ , which cannot be a power law of  $r$ .

	$T^b < \frac{1}{\kappa^b - 1}$	$T^b = \frac{1}{\kappa^b - 1}$	$T^b > \frac{1}{\kappa^b - 1}$
$T^i < \frac{1}{\kappa^i - 1}$		$I_{\max} \propto r I_{\max}^b$ $I_{\max}^b \propto r R_{\text{final}}^b$	$I_{\max} \propto r I_{\max}^b$ $I_{\max}^b \propto 1$
$T^i = \frac{1}{\kappa^i - 1}$	$I_{\max} \propto r R_{\text{final}}^b$	$I_{\max} \propto r R_{\text{final}}^b$	$I_{\max} \propto r R_{\text{final}}^b$

TABLE I: Dependence of  $I_{\max}$  and  $I_{\max}^b$  in different regimes, as  $r \rightarrow 0$ .

	$T^b < \frac{1}{\kappa^b - 1}$	$T^b = \frac{1}{\kappa^b - 1}$	$T^b > \frac{1}{\kappa^b - 1}$
$T^i < \frac{1}{\kappa^i - 1}$		$R_{\text{final}} \propto r R_{\text{final}}^b$ $R_{\text{final}}^b \propto (R_{\text{final}})^{\tau^b - 2}$	$R_{\text{final}} \propto r R_{\text{final}}^b$ $R_{\text{final}}^b \propto 1$
$T^i = \frac{1}{\kappa^i - 1}$	$R_{\text{final}} \propto (r R_{\text{final}}^b)^{\tau^i - 2}$ $R_{\text{final}}^b \propto R_{\text{final}}$	$R_{\text{final}} \propto (r R_{\text{final}}^b)^{\tau^i - 2}$ $R_{\text{final}}^b \propto (R_{\text{final}})^{\tau^b - 2}$	$R_{\text{final}} \propto (r R_{\text{final}}^b)^{\tau^i - 2}$ $R_{\text{final}}^b \propto 1$

TABLE II: Dependence of  $R_{\text{final}}$  and  $R_{\text{final}}^b$  in different regimes, as  $r \rightarrow 0$  [14].

All the scaling relations are summarized in Table I. Combined with previously known results (Table II), we can find the asymptotic dependence of  $I_{\max}$  on  $r$ , as shown in Table III, that gives the power-law exponent  $\epsilon_I$  as in  $I_{\max} \propto r^{1/\epsilon_I}$  in different regimes, as  $r \rightarrow 0$ .

The results can be verified by comparing with the numerical solutions from the EBCM. As in Fig. 3, in a system where both communities and bridge links are ER networks (ER-ER system) such that  $\tau^i = \tau^b = 5/2$ , numerical solutions of Eqs. (2)-(11) are plotted in solid lines, and the dashed lines are straight lines whose slopes are given by Table III. It is clear that the numerical solutions agree with our prediction, as  $r \rightarrow 0$ . Our results also apply to SF networks with  $3 < \lambda < 4$ . As in Fig. 4, in a system where both communities and bridge links are SF networks (SF-SF system) with  $\lambda^i = 3.3$  and  $\lambda^b = 3.4$ , such that  $\tau^i = 36/13$  and  $\tau^b = 19/7$ , numerical solutions of Eqs. (2)-(11) are plotted in solid lines, and the dashed lines are straight lines predicted by Table III. It is clear that the numerical solutions also agree with our prediction for SF networks as  $r \rightarrow 0$ .

	$T^b < \frac{1}{\kappa^b - 1}$	$T^b = \frac{1}{\kappa^b - 1}$	$T^b > \frac{1}{\kappa^b - 1}$
$T^i < \frac{1}{\kappa^i - 1}$	$\emptyset$ (Regime I)	$\epsilon_I = \frac{1 - (\tau^b - 2)}{2 - (\tau^b - 2)}$ (Regime II)	$\epsilon_I = 1$ (Regime III)
$T^i = \frac{1}{\kappa^i - 1}$	$\epsilon_I = 1 - (\tau^i - 2)$ (Regime IV)	$\epsilon_I = 1 - (\tau^i - 2)(\tau^b - 2)$ (Regime V)	$\epsilon_I = 1$ (Regime VI)
$T^i > \frac{1}{\kappa^i - 1}$	$\emptyset$ (Regime VII)	$\emptyset$ (Regime VII)	$\emptyset$ (Regime VII)

TABLE III: Power-law exponent  $\epsilon_I$  as in  $I_{\max} \propto r^{1/\epsilon_I}$  in different regimes, as  $r \rightarrow 0$ .  $\emptyset$  denotes that there is no power-law relation in that regime.

Similar to our previous results for  $R_{\text{final}}$  [14], it can be verified that for all ER networks or SF networks with  $3 < \lambda < 4$ ,  $\epsilon_I$  has a smaller value in regions with smaller transmissibilities ( $T^i$  or  $T^b$ ), so that the curve of  $I_{\max}$  vs.  $r$  goes steeper when  $r$  is small. That is to say, strategies to reduce  $r$  are more effective in controlling peak infection rate, if adequate actions are also taken to reduce  $T^i$  or  $T^b$ . Our results also show that, compared to the values of  $\epsilon_R$  as in  $R_{\text{final}} \propto r^{1/\epsilon_R}$  in each regime [14],  $\epsilon_I$  is either smaller than or equal to  $\epsilon_R$  for all ER networks or SF networks with  $3 < \lambda < 4$ . In general, as  $r$  decreases,  $I_{\max}$  decays faster than  $R_{\text{final}}$  does, i.e., the peak infection rate  $I_{\max}$  responds more sensitively to  $r$  than the total fraction of infection  $R_{\text{final}}$ . Strategies that reduce  $r$  are more crucial, if controlling peak infection rate is prioritized, e.g., if medical resources are limited.

#### IV. CROSSOVERS FOR $T^i \lesssim 1/(\kappa^i - 1)$ WHEN $T^b = 1/(\kappa^b - 1)$

Besides the asymptotic behaviors of  $I_{\max}$  as  $r \rightarrow 0$ , we are expecting crossovers for  $I_{\max}$  between regimes if  $r$  is not small enough, especially when  $T^i \lesssim 1/(\kappa^i - 1)$ . While Regime I is not an epidemic phase, and the values of  $\epsilon_I$  in Regime III and VI are the same, we will only look at the case when  $T^b = 1/(\kappa^b - 1)$ .

When  $T^i \lesssim 1/(\kappa^i - 1)$ , the relation between  $I_{\max}$  and  $r$  behaves differently on both sides of the crossover for two reasons. Firstly, the behavior of  $I_{\max}$  depends on the behavior of  $R_{\text{final}}^b$ , and as discussed in Ref. [14], there is a crossover for  $R_{\text{final}}^b$ . This crossover  $r_1^*$  is determined by  $1/s_{\max} \sim r_1^*(R_{\text{final}}^b)^*$ , and thus we get the first crossover point  $r_1^* \sim |T^i - \frac{1}{\kappa^i - 1}|^{[1 - (\tau^i - 2)(\tau^b - 2)]/\sigma}$

when  $T^b = 1/(\kappa^b - 1)$ . Secondly, whether  $I_{\max}$  depends on  $R_{\text{final}}^b$  or  $I_{\max}^b$  is determined by how the time scale of a community is compared with that of the whole system. In this case, the turning point occurs when the time scale of a community is approximately the same as the time scale of the system, i.e.,  $|T^i - \frac{1}{\kappa^i - 1}|^{-z^i \nu^i} \sim |T^b - T_c^b|^{-z^b \nu^b}$ , which reduces to  $|T^i - \frac{1}{\kappa^i - 1}| \sim |T^b - T_c^b|$  for ER and SF networks with  $3 < \lambda < 4$ , where  $T_c^b$  is the critical value of bridge link transmissibility  $T^b$  for the whole system, given a fixed value of  $T^i$ . Then we have the second crossover point (see Appendix B for details)

$$\left| T^i - \frac{1}{\kappa^i - 1} \right| \sim \frac{\langle k^i \rangle \langle k^b \rangle T^i}{(\kappa^i - 1)(\kappa^b - 1)^2 \left( \frac{1}{\kappa^i - 1} - T^i \right)} \cdot r_2^*, \quad (1)$$

which gives  $r_2^* \sim |T^i - \frac{1}{\kappa^i - 1}|^2$ .

In summary, when  $T^i \lesssim 1/(\kappa^i - 1)$  and  $T^b = 1/(\kappa^b - 1)$ , we expect crossovers in the relation between  $I_{\max}$  and  $r$ . If  $r$  is small enough so that  $r < r_1^*$  and  $r < r_2^*$ ,  $I_{\max}$  vs.  $r$  follows its asymptotic behavior as  $T^i < 1/(\kappa^i - 1)$ , while if  $r$  is larger than both  $r_1^*$  and  $r_2^*$ , the relation between  $I_{\max}$  and  $r$  will be as if  $T^i = 1/(\kappa^i - 1)$ , both of which can be verified by the numerical solutions from Eqs. (2)-(11), as shown in Fig. 5. Moreover, we can also see a transition part when  $r_2^* < r < r_1^*$ , whose slope can also be predicted by combining dependencies of  $R_{\text{final}}$  and  $I_{\max}$  with  $r$  from different regimes.

Practically, when actions are taken to reduce  $r$ , it is essential to know that the peak infection rate  $I_{\max}$  may not be reduced immediately as fast as the predicted behaviors for asymptotic situations. This is due to the fact that  $r$  may be not small enough, and we are on the right side of the crossovers. However, we would expect  $I_{\max}$  to drop down as fast as predicted, once  $r$  goes below the crossover points. Our results enable us to find the balance between relieving medical pressure and reopening, and to make better plans for epidemic strategies.

## V. CONCLUSIONS

In this paper, we study the dynamic properties of a two-community system with bridge nodes, especially how the peak infection rate  $I_{\max}$  depends on the fraction of bridge nodes  $r$ . We find the asymptotic relation between  $I_{\max}$  and  $r$  to have power-law behaviors in multiple regimes, and analytically calculate the power-law exponents for each regime, which are verified by numerical solutions from the EBCM. We also find crossovers between regimes

when  $T^i \lesssim 1/(\kappa^i - 1)$  and  $T^b = 1/(\kappa^b - 1)$ , if  $r$  is not small enough, which can be explained by the comparison of time scales between different parts of the system. Our methodology can be easily extended to situations with multiple communities, or communities with different internal degree distributions, or different internal transmissibilities.

The results can be very instructive for making epidemic strategies, e.g., to anticipate the effectiveness of a strategy, and to find the best practice of reopening under the premise that all patients can get timely treatment.

## VI. ACKNOWLEDGMENTS

J.M. and L.A.B. acknowledge support from DTRA Grant No. 9500309448. X.M. was supported by the NetSeed: Seedling Research Award of the Network Science Institute of Northeastern University. L.A.B. wish to thank UNMdP (EXA 956/20) and FONCyT (PICT 1422/2019) for financial support.

### A. EBCM ADAPTED TO THE SIR MODEL

The Edge-Based Compartmental Model (EBCM) adapted to the SIR model was introduced in Ref. [18], and was further discussed for multi-community networks with bridge nodes in Ref. [19]. In this model, two auxiliary variables  $\theta^i(t), \theta^b(t)$  are defined as the probabilities that the disease has not been transmitted through a randomly chosen internal or bridge link from a node, respectively, by time  $t$ , which could fall into one of the three categories: the node is still susceptible (S) up to this instant (with probability  $\Phi_S(t)$ ), the node is infected (I) at this instant but has not transmitted through this link yet (with probability  $\Phi_I(t)$ ), or the node is already recovered (R) and has never transmitted the disease through this link (with probability  $\Phi_R(t)$ ) [19]. The time dependence of all variables of the SIR model can then be calculated numerically from [19]:

$$\theta^i(t+1) = \theta^i(t) - q^i \Phi_I^i(t) \quad (2)$$

$$\theta^b(t+1) = \theta^b(t) - q^b \Phi_I^b(t) \quad (3)$$

$$\begin{aligned} \Delta \Phi_S^i(t) = (1-r) [G_1^i(\theta^i(t+1)) - G_1^i(\theta^i(t))] \\ + r [G_1^i(\theta^i(t+1))G_0^b(\theta^b(t+1)) - G_1^i(\theta^i(t))G_0^b(\theta^b(t))] \end{aligned} \quad (4)$$

$$\Delta \Phi_S^b(t) = G_0^i(\theta^i(t+1))G_1^b(\theta^b(t+1)) - G_0^i(\theta^i(t))G_1^b(\theta^b(t)) \quad (5)$$

$$\Delta \Phi_I^i(t) = -q^i \Phi_I^i(t) - \Delta \Phi_S^i(t) + (1-T^i)\Delta \Phi_S^i(t-t_r) \quad (6)$$

$$\Delta \Phi_I^b(t) = -q^b \Phi_I^b(t) - \Delta \Phi_S^b(t) + (1-T^b)\Delta \Phi_S^b(t-t_r) \quad (7)$$

$$\Delta S^i(t) = (1-r) [G_0^i(\theta^i(t+1)) - G_0^i(\theta^i(t))] \quad (8)$$

$$\Delta S^b(t) = r [G_0^i(\theta^i(t+1))G_0^b(\theta^b(t+1)) - G_0^i(\theta^i(t))G_0^b(\theta^b(t))] \quad (9)$$

$$\Delta I^i(t) = -\Delta S^i(t) + \Delta S^i(t-t_r) \quad (10)$$

$$\Delta I^b(t) = -\Delta S^b(t) + \Delta S^b(t-t_r) \quad (11)$$

where  $q^i$  (or  $q^b$ ) is the probability that an infected node transmits the disease to its susceptible neighbor through an internal link (or a bridge link) at each time step, and  $t_r$  is the number of time steps it takes for an infected individual to recover, and thus  $T^i = 1 - (1 - q^i)^{t_r}$  and  $T^b = 1 - (1 - q^b)^{t_r}$ .

Equations (2)-(3) are due to the fact that the disease can only get transmitted through a link when the node is infected. In Eqs. (4)-(5) and (8)-(9),  $\Phi_S^i$  or  $\Phi_S^b$  is calculated by the probability that the disease has not transmitted to the node through any other links by time  $t$ , and  $S^i$  or  $S^b$  is calculated by the probability that the disease has not transmitted to the node through any of its links by time  $t$ . Eqs. (6)-(7) and (10)-(11) take  $\Delta\theta(t) = \Delta\Phi_S(t) + \Delta\Phi_I(t) + \Delta\Phi_R(t)$  and  $0 = \Delta S + \Delta I + \Delta R$  into account, and that all infected nodes will recover after  $t_r$  time steps, so that  $\Delta\Phi_R(t) = -\Delta\Phi_S(t-t_r)$  and  $\Delta R(t) = -\Delta S(t-t_r)$ .

## B. DERIVATION OF $T_c^b$ FOR THE WHOLE SYSTEM GIVEN A FIXED $T^i$

By mapping the final state of the whole system to the giant component in the link percolation process, we have the self-consistent equations [14]

$$f^i = (1-r) [1 - G_1^i(1 - T^i f^i)] + r [1 - G_1^i(1 - T^i f^i)G_0^b(1 - T^b f^b)], \quad (12)$$

$$f^b = 1 - G_0^i(1 - T^i f^i)G_1^b(1 - T^b f^b), \quad (13)$$

where  $f^i$  or  $f^b$  is the probability to expand a branch to the infinity through an internal link or a bridge link, respectively.

The critical value of  $T^b$  given  $T^i$  can be solved by letting the Jacobian matrix satisfy  $|J - I|_{f^i, f^b=0} = 0$ , where  $J_{i,j} = \frac{\partial f_i}{\partial f_j}$ , in which each of  $f_i$  and  $f_j$  represents  $f^i$  or  $f^b$ . Thus, we have

$$\begin{vmatrix} T^i(\kappa^i - 1) - 1 & rT_c^b \langle k^b \rangle \\ T^i \langle k^i \rangle & T_c^b(\kappa^b - 1) - 1 \end{vmatrix} = 0. \quad (14)$$

So  $T_c^b$  is given by

$$T_c^b = \frac{(\kappa^i - 1)T^i - 1}{(\kappa^b - 1)[(\kappa^i - 1)T^i - 1] - r \langle k^i \rangle \langle k^b \rangle T^i}. \quad (15)$$

When  $r$  is small, this expression can be approximated by looking only at the first two orders of its Taylor series expansion around  $r = 0$ . The zeroth order gives

$$T_c^b|_{r=0} = \frac{1}{\kappa^b - 1}, \quad (16)$$

while the first order derivative is

$$\begin{aligned} \left. \frac{\partial T_c^b}{\partial r} \right|_{r=0} &= \left. \frac{[(\kappa^i - 1)T^i - 1] \langle k^i \rangle \langle k^b \rangle T^i}{[(\kappa^b - 1)[(\kappa^i - 1)T^i - 1] - r \langle k^i \rangle \langle k^b \rangle T^i]^2} \right|_{r=0} \\ &= \frac{\langle k^i \rangle \langle k^b \rangle T^i}{(\kappa^b - 1)^2 [(\kappa^i - 1)T^i - 1]} \\ &= -\frac{\langle k^i \rangle \langle k^b \rangle T^i}{(\kappa^i - 1)(\kappa^b - 1)^2 \left[ \frac{1}{\kappa^i - 1} - T^i \right]}. \end{aligned} \quad (17)$$

Thus, we have

$$T_c^b \approx \frac{1}{\kappa^b - 1} - \frac{\langle k^i \rangle \langle k^b \rangle T^i}{(\kappa^i - 1)(\kappa^b - 1)^2 \left[ \frac{1}{\kappa^i - 1} - T^i \right]} \cdot r. \quad (18)$$

### C. $I_{\max}$ WITH $n$ PATIENT ZEROS IN AN ISOLATED NETWORK

In the case where a disease starts spreading from one patient, i.e., ‘‘patient zero’’, in an isolated network, there are behaviors around criticality  $\langle s \rangle \sim |T - T_c|^{-\gamma}$ , where  $\langle s \rangle$  represents the mean cluster size,  $l \sim |T - T_c|^{-z\nu}$ , where  $l$  represents the chemical distance or shortest-path distance, and thus  $\langle s \rangle \sim l^{\gamma/z\nu}$ . Considering  $\langle s \rangle \sim \int N(l)dl$  and  $I \sim N(l)$ , we have  $I \sim l^{\gamma/z\nu-1}$  [17], which becomes  $I \sim O(1)$  for both ER and SF networks with  $3 < \lambda < 4$ , whose  $\gamma = 1$ ,  $z = 2$  and  $\nu = 1/2$  [23].

For epidemics starting from  $n$  patient zeros simultaneously in an isolated network,  $I$  would be less than  $n \cdot O(1)$  with time going on, if the spreading paths from different patient zeros overlap. Due to the initial condition  $I_0 = n$ , we will have  $I_{\max} \propto n$ .

---

- [1] M. E. Newman, *Physical Review E* **66**, 016128 (2002).
- [2] R. Cohen, K. Erez, S. Havlin, M. E. Newman, A.-L. Barabási, D. J. Watts, *et al.*, in *The Structure and Dynamics of Networks* (Princeton University Press, 2011) pp. 507–509.
- [3] M. E. Newman, S. H. Strogatz, and D. J. Watts, *Physical Review E* **64**, 026118 (2001).
- [4] D. S. Callaway, M. E. Newman, S. H. Strogatz, and D. J. Watts, *Physical Review Letters* **85**, 5468 (2000).
- [5] P. Grassberger, *Mathematical Biosciences* **63**, 157 (1983).
- [6] M. E. Newman, *Networks* (Oxford University Press, 2010).
- [7] D. Stauffer and A. Aharony, *Introduction to percolation theory* (Taylor & Francis, 2018).
- [8] S. V. Buldyrev, R. Parshani, G. Paul, H. E. Stanley, and S. Havlin, *Nature* **464**, 1025 (2010).
- [9] I. Kryven, *Nat. Commun.* **10**, 1 (2019).
- [10] J. Gao, S. V. Buldyrev, S. Havlin, and H. E. Stanley, *Physical Review Letters* **107**, 195701 (2011).
- [11] D. Y. Kenett, J. Gao, X. Huang, S. Shao, I. Vodenska, S. V. Buldyrev, G. Paul, H. E. Stanley, and S. Havlin, in *Networks of Networks: The Last Frontier of Complexity* (Springer, 2014) pp. 3–36.
- [12] J. Gao, S. V. Buldyrev, H. E. Stanley, X. Xu, and S. Havlin, *Physical Review E* **88**, 062816 (2013).
- [13] G. Dong, J. Fan, L. M. Shekhtman, S. Shai, R. Du, L. Tian, X. Chen, H. E. Stanley, and S. Havlin, *Proceedings of the National Academy of Sciences* **115**, 6911 (2018).
- [14] J. Ma, L. D. Valdez, and L. A. Braunstein, *Physical Review E* **102**, 032308 (2020).
- [15] P. Leath, *Physical Review B* **14**, 5046 (1976).
- [16] Z. Alexandrowicz, *Physics Letters A* **80**, 284 (1980).
- [17] Z. Zhou, J. Yang, Y. Deng, and R. M. Ziff, *Physical Review E* **86**, 061101 (2012).
- [18] J. C. Miller, A. C. Slim, and E. M. Volz, *Journal of the Royal Society Interface* **9**, 890 (2012).

- [19] L. D. Valdez, H. A. Rêgo, H. E. Stanley, S. Havlin, and L. A. Braunstein, *New Journal of Physics* **20**, 125003 (2018).
- [20] C. Lagorio, M. Dickison, F. Vazquez, L. A. Braunstein, P. A. Macri, M. Migueles, S. Havlin, and H. E. Stanley, *Physical Review E* **83**, 026102 (2011).
- [21] C. Buono, L. G. Alvarez-Zuzek, P. A. Macri, and L. A. Braunstein, *PLoS ONE* **9**, e92200 (2014).
- [22] R. Cohen, D. ben-Avraham, and S. Havlin, *Physical Review E* **66**, 036113 (2002).
- [23] R. Cohen, S. Havlin, and D. ben-Avraham, *Handbook of Graphs and Networks* **4** (2003).
- [24] P. Grassberger, *Journal of Physics A: Mathematical and General* **25**, 5475 (1992).

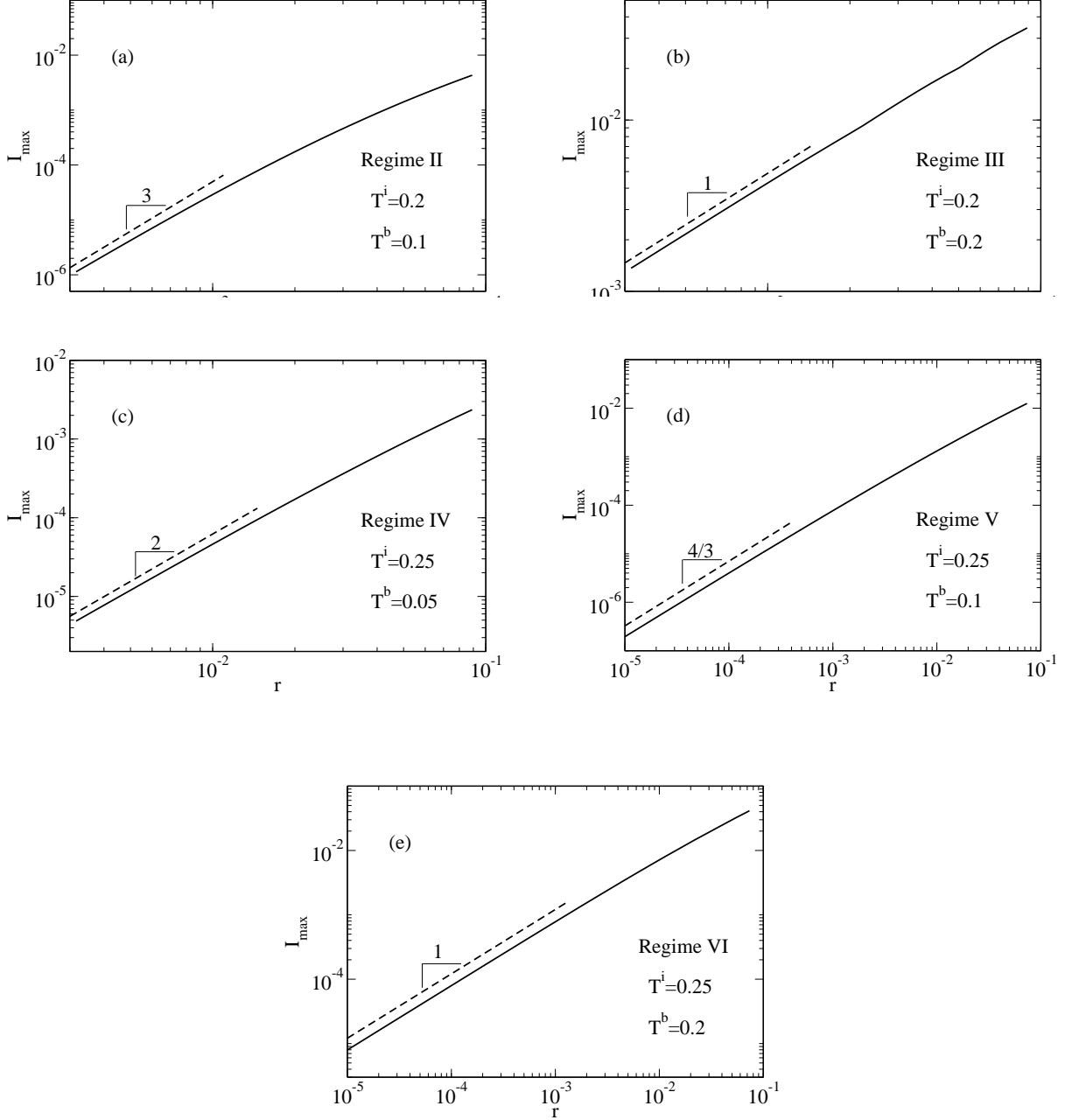


FIG. 3:  $I_{\max}$  as a function of  $r$  for different regimes in a ER-ER system where a power law exists: (a) Regime II:  $T^i = 0.2$ ,  $T^b = 0.1$ ; (b) Regime III:  $T^i = 0.2$ ,  $T^b = 0.2$ ; (c) Regime IV:  $T^i = 0.25$ ,  $T^b = 0.05$ ; (d) Regime V:  $T^i = 0.25$ ,  $T^b = 0.1$ ; and (e) Regime VI:  $T^i = 0.25$ ,  $T^b = 0.2$ . Both internal links and bridge links are ER networks, with  $\langle k^i \rangle = 4$  and  $\langle k^b \rangle = 10$ , such that  $1/(\kappa^i - 1) = 0.25$  and  $1/(\kappa^b - 1) = 0.1$ , respectively. In each regime, numerical solutions of Eqs. (2)-(11) are plotted in solid lines, and dashed lines represent slopes predicted by Table III.

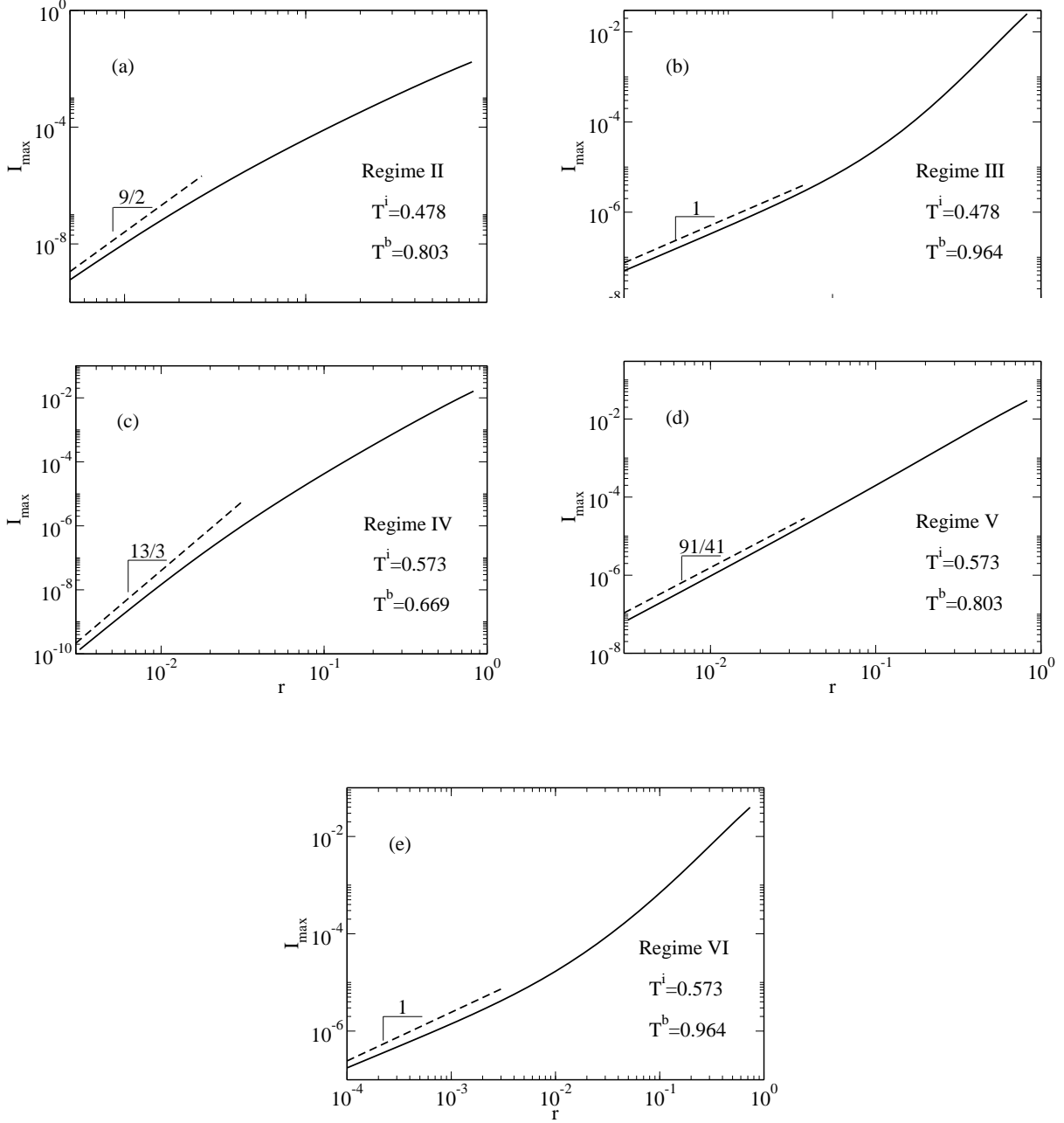


FIG. 4:  $I_{\max}$  as a function of  $r$  for different regimes in an SF-SF system where a power law exists: (a) Regime II:  $T^i = 0.478$ ,  $T^b = 0.803$ ; (b) Regime III:  $T^i = 0.478$ ,  $T^b = 0.964$ ; (c) Regime IV:  $T^i = 0.573$ ,  $T^b = 0.669$ ; (d) Regime V:  $T^i = 0.573$ ,  $T^b = 0.803$ ; and (e) Regime VI:  $T^i = 0.573$ ,  $T^b = 0.964$ . Both internal links and bridge links are SF networks, with  $\lambda^i = 3.3$  and  $\lambda^b = 3.4$ , such that  $\tau^i = 36/13$ ,  $\tau^b = 19/7$ ,  $1/(\kappa^i - 1) = 0.573$ , and  $1/(\kappa^b - 1) = 0.803$ , respectively. In each regime, numerical solutions of Eqs. (2)-(11) are plotted in solid lines, and dashed lines represent slopes predicted by Table III.

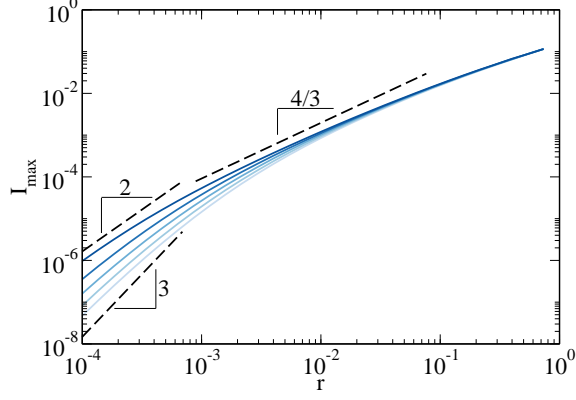


FIG. 5: Crossovers of  $I_{\max}$  as a function of  $r$  when  $T^i \lesssim 1/(\kappa^i - 1)$ , i.e.,  $T^i = 0.245, 0.246, 0.247, 0.248, 0.249$  (from light blue to dark blue), with  $T^b = 1/(\kappa^b - 1) = 0.1$ . Both internal links and bridge links are ER networks, with  $\langle k^i \rangle = 4$  and  $\langle k^b \rangle = 10$ , respectively. Dashed lines represent slopes predicted by Tables I and II for different regimes.